Preparation, structural and optical characterization of nanocrystalline ZnO doped with luminescent Ag-nanoclusters

A. S. Kuznetsov,[1] Y-G. Lu,[2] S. Turner,[2] M. V. Shestakov,[1,3] V. K. Tikhomirov,[1,*] D. Kirilenko,[2] J. Verbeeck,[2] A. N. Baranov,[4] and V. V. Moshchalkov[1]

[1]*INPAC-Institute for Nanoscale Physics and Chemistry, Katholieke Universiteit Leuven, Belgium*
[2]*EMAT, Electron Microscopy for Materials Science, Universiteit Antwerpen, Belgium*
[3]*Department of Materials Science, Lomonosov Moscow State University, Moscow, Russian Federation*
[4]*Department of Chemistry, Lomonosov Moscow State University, Moscow, Russian Federation*
**Victor.Tikhomirov@fys.kuleuven.be*

Abstract: Nanocrystalline ZnO doped with Ag-nanoclusters has been synthesized by a salt solid state reaction. Three overlapping broad emission bands due to the Ag nanoclusters have been detected at about 570, 750 and 900 nm. These emission bands are excited by an energy transfer from the exciton state of the ZnO host when pumped in the wavelength range from 250 to 400 nm. The 900 nm emission band shows characteristic orbital splitting into three components pointing out that the anisotropic crystalline wurtzite host of ZnO is responsible for this feature. Heat-treatment and temperature dependence studies confirm the origin of these emission bands. An energy level diagram for the emission process and a model for Ag nanoclusters sites are suggested. The emission of nanocrystalline ZnO doped with Ag nanoclusters may be applied for white light generation, displays driven by UV light, down-convertors for solar cells and luminescent lamps.

OCIS codes: (160.4236) Nanomaterials; (250.5230) Photoluminescence; (160.6000) Semiconductor materials.

References and links

1. C. Klingshirn, "ZnO: From basics towards applications," Phys. Status Solidi B **244**(9), 3027–3073 (2007).
2. Ü. Özgür, Y. I. Alivov, C. Liu, A. Teke, M. A. Reshchikov, S. Doğan, V. Avrutin, S.-J. Cho, and H. Morkoç, "A comprehensive review of ZnO materials and devices," J. Appl. Phys. **98**(4), 041301 (2005).
3. Ü. Özgür, D. Hofstetter, and H. Morkoç, "ZnO devices and applications: a review of current status and future prospects," Proc. IEEE **98**(7), 1255–1268 (2010).
4. A. Baltakesmez, S. Tekmen, and S. Tüzemen, "ZnO homojunction white light-emitting diodes," J. Appl. Phys. **110**(5), 054502 (2011).
5. K. S. Leschkies, R. Divakar, J. Basu, E. Enache-Pommer, J. E. Boercker, C. B. Carter, U. R. Kortshagen, D. J. Norris, and E. S. Aydil, "Photosensitization of ZnO nanowires with CdSe quantum dots for photovoltaic devices," Nano Lett. **7**(6), 1793–1798 (2007).
6. L. Lu, R. Li, K. Fan, and T. Peng, "Effects of annealing conditions on the photoelectrochemical properties of dye-sensitized solar cells made with ZnO nanoparticles," Sol. Energy **84**(5), 844–853 (2010).
7. I. Repins, M. A. Contreras, B. Egaas, C. DeHart, J. Scharf, C. L. Perkins, B. To, and R. Noufi, "19.9%-efficient ZnO/CdS/$CuInGaSe_2$ solar cell with 81.2% fill factor," Prog. Photovolt. Res. Appl. **16**(3), 235–239 (2008).
8. I. Hussain, N. Bano, S. Hussain, O. Nur, and M. Willander, "Study of intrinsic white light emission and its components from ZnO-nanorods/p-polymer hybrid junctions grown on glass substrates," J. Mater. Sci. **46**(23), 7437–7442 (2011).
9. S. Fujihara, Y. Ogawa, and A. Kasai, "Tunable visible photoluminescence from ZnO thin films through Mg-doping and annealing," Chem. Mater. **16**(15), 2965–2968 (2004).
10. E. M. Wong and P. C. Searson, "ZnO quantum particle thin films fabricated by electrophoretic deposition," Appl. Phys. Lett. **74**(20), 2939–2941 (1999).
11. A. Janotti and C. G. Van de Walle, "Fundamentals of zinc oxide as a semiconductor," Rep. Prog. Phys. **72**(12), 126501 (2009).
12. M. V. Shestakov, V. K. Tikhomirov, D. Kirilenko, A. S. Kuznetsov, L. F. Chibotaru, A. N. Baranov, G. Van Tendeloo, and V. V. Moshchalkov, "Quantum cutting in Li (770 nm) and Yb (1000 nm) co-dopant emission bands by energy transfer from the ZnO nano-crystalline host," Opt. Express **19**(17), 15955–15964 (2011).

#166060 - $15.00 USD Received 3 Apr 2012; revised 16 Apr 2012; accepted 16 Apr 2012; published 30 Apr 2012

13. M. V. Shestakov, A. N. Baranov, Y. V. Zubavichus, V. K. Tikhomirov, A. S. Kuznetsov, A. A. Veligzhanin, A. Y. Kharin, V. Y. Timoshenko, and V. V. Moshchalkov (Catholic University, Leuven) are preparing a manuscript to be called "Preparation and energy transfer luminescence of nanocrystalline ZnO:Yb^{3+}."
14. Y.-C. Lee, S.-Y. Hu, W. Water, K.-K. Tiong, Z.-C. Feng, Y.-T. Chen, J.-C. Huang, J.-W. Lee, C.-C. Huang, J.-L. Shen, and M.-H. Cheng, "Rapid thermal annealing effects on the structural and optical properties of ZnO films deposited on Si substrates," J. Lumin. **129**(2), 148–152 (2009).
15. I. Díez and R. H. A. Ras, "Fluorescent silver nanoclusters," Nanoscale **3**(5), 1963–1970 (2011).
16. V. K. Tikhomirov, V. D. Rodríguez, A. S. Kuznetsov, D. Kirilenko, G. Van Tendeloo, and V. V. Moshchalkov, "Preparation and luminescence of bulk oxyfluoride glasses doped with Ag nanoclusters," Opt. Express **18**(21), 22032–22040 (2010).
17. A. S. Kuznetsov, N. T. Cuong, V. K. Tikhomirov, M. Jivanescu, A. Stesmans, L. F. Chibotaru, J. J. Velázquez, V. D. Rodríguez, D. Kirilenko, G. Van Tendeloo, and V. V. Moshchalkov, "Effect of heat-treatment on luminescence and structure of Ag nanoclusters doped oxyfluoride glasses and implication for fiber drawing," Opt. Mater. **34**(4), 616–621 (2012).
18. S. Suwanboon, P. Amornpitoksuk, and A. Sukolrat, "Dependence of optical properties on doping metal, crystallite size and defect concentration of M-doped ZnO nanopowders (M = Al, Mg, Ti)," Ceram. Int. **37**(4), 1359–1365 (2011).
19. S. T. Kuo, W. H. Tuan, J. Shieh, and S. F. Wang, "Effect of Ag on the microstructure and electrical properties of ZnO," J. Eur. Ceram. Soc. **27**(16), 4521–4527 (2007).
20. Y. Chen, X. L. Xu, G. H. Zhang, H. Xue, and S. Y. Ma, "A comparative study of the microstructures and optical properties of Cu- and Ag-doped ZnO thin films," Physica B **404**(20), 3645–3649 (2009).
21. R. T. Sapkal, S. S. Shinde, A. R. Babar, A. V. Moholkar, K. Y. Rajpure, and C. H. Bhosale, "Structural, morphological, optical and photoluminescence properties of Ag-doped zinc oxide thin films," Mater. Express **2**(1), 64–70 (2012).
22. L.-N. Wang, L.-Z. Hu, H.-Q. Zhang, Y. Qiu, Y. Lang, G.-Q. Liu, G.-W. Qu, J.-Y. Ji, and J.-X. Ma, "Effect of substrate temperature on the structural and Raman properties of Ag-doped ZnO films," Chin. Phys. Lett. **29**(1), 017302 (2012).
23. G. Chai, C. Lin, J. Wang, M. Zhang, J. Wei, and W. Cheng, "Density functional theory simulations of structures and properties for Ag-doped ZnO nanotubes," J. Phys. Chem. C **115**(7), 2907–2913 (2011).
24. R. M. Farrell, E. C. Young, F. Wu, S. P. DenBaars, and J. S. Speck, "Materials and growth issues for high-performance nonpolar and semipolar light-emitting devices," Semicond. Sci. Technol. **27**(2), 024001 (2011).
25. E. Rangel, E. Matioli, Y.-S. Choi, C. Weisbuch, J. S. Speck, and E. L. Hu, "Directionality control through selective excitation of low-order guided modes in thin-film InGaN photonic crystal light-emitting diodes," Appl. Phys. Lett. **98**(8), 081104 (2011).
26. X.-H. Li, R. Song, Y.-K. Ee, P. Kumnorkaew, J. F. Gilchrist, and N. Tansu, "Light extraction efficiency and radiation patterns of III-Nitride light-emitting diodes with colloidal microlens arrays with various aspect ratios," IEEE Photonics J. **3**(3), 489–499 (2011).
27. C. W. Chen, S. C. Hung, C. H. Lee, C. J. Tun, C. H. Kuo, M. D. Yang, C. W. Yeh, C. H. Wu, and G. C. Chi, "Nonpolar light emitting diode made by m-plane n-ZnO/p-GaN heterostructure," Opt. Mater. Express **1**(8), 1555–1560 (2011).
28. A. N. Baranov, G. N. Panin, T. W. Kang, and Y.-J. Oh, "Growth of ZnO nanorods from a salt mixture," Nanotechnology **16**(9), 1918–1923 (2005).
29. A. N. Baranov, C. H. Chang, O. A. Shlyakhtin, G. N. Panin, T. W. Kang, and Y.-J. Oh, "In situ study of the ZnO–NaCl system during the growth of ZnO nanorods," Nanotechnology **15**(11), 1613–1619 (2004).
30. S. Ye, N. Jiang, F. He, X. Liu, B. Zhu, Y. Teng, and J. R. Qiu, "Intense near-infrared emission from ZnO-$LiYbO_2$ hybrid phosphors through efficient energy transfer from ZnO to Yb^{3+}," Opt. Express **18**(2), 639–644 (2010).
31. Y. Teng, J. Zhou, X. Liu, S. Ye, and J. Qiu, "Efficient broadband near-infrared quantum cutting for solar cells," Opt. Express **18**(9), 9671–9676 (2010).
32. V. V. Osiko, "Low-temperature luminescence of zinc oxide in the infrared region of the spectrum," Opt. Spectrosc. **7**, 770–775 (1959).
33. Y. M. Gerbshtein and Y. M. Zelikin, "On the red luminescence band of zinc oxide," Opt. Spectrosc. **28**, 521–522 (1970).
34. J. Zheng, P. R. Nicovich, and R. M. Dickson, "Highly fluorescent noble-metal quantum dots," Annu. Rev. Phys. Chem. **58**(1), 409–431 (2007).
35. J. C. Pickering and V. Zilio, "New accurate data for the spectrum of neutral silver," Eur. Phys. J. D **13**(2), 181–185 (2001).
36. A. S. Sugano, Y. Tanabe, and H. Kamimura, *Multiplets of Transition-Metal Ion in Crystal* (Academic Press, New York, London, 1970).
37. C. J. Ballhausen, *Introduction to Ligand Field Theory* (McGraw-Hill, New York, 1990).
38. T. Hirai, Y. Harada, S. Hashimoto, T. Itoh, and N. Ohno, "Luminescence of excitons in mesoscopic ZnO particles," J. Lumin. **112**(1-4), 196–199 (2005).

1. Introduction

Zinc oxide (ZnO) is a wide band gap II-VI semiconductor with band gap of 3.4 eV and large exciton binding energy of 60 meV. It is used for example in transparent electrodes [1], liquid

#166060 - $15.00 USD Received 3 Apr 2012; revised 16 Apr 2012; accepted 16 Apr 2012; published 30 Apr 2012

crystals displays and LEDs [1–3] and solar cells [4–7]. ZnO is now also being investigated for UV driven white light generation [3,4,8], tunable light sources [9], nano-lasing [1,2], green phosphors [3,4] and optical non-linear applications [10]. Exciton photoluminescence from ZnO is observed around 380 nm [1,11]. ZnO also emits intrinsic luminescence in the green spectral range with a minor emission tail extending down to the red. This emission originates from deep defects, such as oxygen and zinc vacancies, and impurities ([1,2] and refs. therein). The emission properties of ZnO can be modified by intentional doping [9,12,13] and post-annealing [14].

In this paper, silver (Ag) has been studied as a dopant for ZnO. Ag *single* atoms are known as commercial blue phosphors with very high luminescence yield for lamps and computer monitor displays. It is also known that Ag atoms can form *luminescent nanoclusters*, which consist of only few Ag-atoms, especially when embedded in liquids/colloids/polymers/zeolites, as discussed e.g. in a recent review ([15] and refs. therein), and more recently in a glassy host [16,17]. The origin of emission of the Ag-nanoclusters is different from the emission of single Ag atoms, and yet it is not understood to date [15].

Recent papers reported on preparation and characterization of Ag-doped ZnO materials [18–23]. An effect of Ag-doping on electrical properties of ZnO was reported in [19]. An effect of Ag doping on the UV exciton emission band of ZnO host has been reported [20–22]. The Ag-doping is found to enhance exciton emission band of ZnO, but no effect on the visible luminescence of ZnO was reported. Quantum chemistry calculations were carried out in [23], which suggested formation of Ag nanoclusters in form of dimers, trimers and tetramers in Ag-doped ZnO single-walled nanotubes.

The Ag-doped ZnO is an alternative to white light LEDs based on InGaN [24–27], which became already a commercial product. Although the quantum yield of InGaN based LEDs approaches a value of up to 70% [24–26], but these light sources have unidirectional emission and still are expensive. Therefore, a cheap solid state lighting based on ZnO:Ag nanopowders omnidirectional emission is sought in this work and it can be used therefore in a wider range of applications including conventional luminescent lamps, displays and solar spectrum down-shifting.

In this article we report, on the preparation of *ZnO nanocrystals doped with Ag-nanoclusters* consisting of few Ag-atoms. Upon Ag doping we observed a significant modification of the intrinsic emission spectrum of ZnO: i) a green band/shoulder around 570 nm, which is red-shifted with respect to an intrinsic band of ZnO host, ii) a red 750 nm band, which is related to Ag-O units/clusters and iii) an infrared 900 nm band, which is orbital split in three components pointing out the crystalline surroundings of the Ag-nanoclusters. The later orbital splitting of the Ag nanoclusters emission band in a crystalline host is reported for the first time, to the best of our knowledge. Photoluminescence excitation spectroscopy revealed that these bands are efficiently excited via exciton state of the ZnO host; i.e. when pumped in the UV-blue range from 250 to 400 nm. It was possible to tune the spectral position and relative emission intensity of the bands by subjecting samples to heat-treatment in oxygen. An energy level diagram for the emission process and a model for the Ag nanoclusters sites are suggested.

This new luminescent Ag-nanoclusters doped ZnO nanocrystals may be a candidate material for down-shifting of the solar spectrum, UV-driven white light generation, tunable phosphors for flexible display and luminescent lamps.

2. Experimental

In this work a salt solid state reaction based on the methods [28,29] was used for preparation of nanocrystalline ZnO powder doped with Ag nanoclusters. The $Zn(NO_3)_2$ and $AgNO_3$ aqueous solutions have been prepared, mixed and precipitated by excessive amounts of aqueous $NaHCO_3$ solution. The Ag concentration was varied from 0 to 1.0 mol%. The precipitated zinc carbonate hydroxide (ZCH) containing Ag dopants was washed by distilled water and freeze dried in a laboratory freeze dryer. Next, the sintering of the ZCH was carried out in a muffle furnace at 700°C during 2 h. The resulting nanopowders have been pressed

#166060 - $15.00 USD Received 3 Apr 2012; revised 16 Apr 2012; accepted 16 Apr 2012; published 30 Apr 2012

into pellets for optical measurements. Some of the samples were subjected to additional heat-treatment in oxygen atmosphere at 700 °C in an oven.

An X-ray diffractometer (XRD) Rigaku was used to characterize the crystal structure of the samples. Transmission electron microscopy (TEM) and high resolution TEM with energy dispersive X-ray spectroscopy (TEM EDX) were applied to identify the nanostructure of the samples and their chemical composition. TEM and EDX investigations were performed on mechanically crushed samples deposited on holey carbon grids using a Tecnai G2 microscope operated at 200 kV, equipped with an energy dispersive X-ray analysis attachment. High resolution high angle annular dark-field scanning transmission electron microscopy (HAADF-STEM) was used to characterize the local nanostructure of the samples. HAADF-STEM images were recorded on an FEI Titan 80-300 "cubed" microscope fitted with an aberration corrector for the probe-forming lens, operated at 120 kV.

Emission spectra were measured using an Andor Technologies Newton DU970 EMCCD camera attached to a Shamrock SR303i spectrometer. Excitation of the emission was done using either a 355 nm (1 mW) monochromatic line of an Ar-ion laser or a tunable Xe (300 W) source. In some experiments, the laser excitation energy was attenuated down to some μW, providing high and low pump power regimes for the measurements, respectively. The tuning of the Xe-source was used also for recording the excitation spectra. Low-temperature measurements were carried out in a helium-flow optical cryostat down to 3.7 K. The spectral response of the equipment was taken into account.

3. Results

3.1 Structural study of the ZnO:Ag nanoparticles

As prepared samples were verified to be wurtzite ZnO based upon their XRD patterns, the examples are shown in Fig. 1. XRD peaks characteristic of the anisotropic wurtzite ZnO lattice can clearly be seen in Fig. 1, while no detectable Ag-crystalline phase can be seen. A low-magnification TEM image of the Ag-doped ZnO nanopowder is shown in Fig. 2(a). The powder consists of ZnO nanoparticles with size of the order of 100-500 nm. Electron diffraction pattern of image of Fig. 2(a) is shown in Fig. 2(b) confirming that the ZnO nanoparticles have a hexagonal wurtzite structure. Figure 2(c) shows an HAADF-STEM image along the $[2\bar{1}\bar{1}0]$ zone axis taken from the edge of one of ZnO nanoparticles. The contrast in this type of image is mass-thickness sensitive; scaling with sample thickness as well as with the atomic number $Z^{\sim 1.7}$. No significant electron contrast differences are observed in Fig. 2(c), even though Ag nanoparticles may show up as bright regions in HAADF-STEM imaging due to the higher average atomic number of Ag compared to ZnO. This may indicate a degree of distribution of outer electron density of Ag in the surroundings.

Even though Ag clusters are not directly observed in HAADF-STEM, e.g. in Fig. 2(c), Ag is clearly present in these ZnO nanoparticles as evidenced by the TEM EDX spectrum in Fig. 3 recorded from the region shown in Fig. 2(a). In particular, the peak around 25 keV in Fig. 3 clearly corresponds to Ag and confirms the presence of silver atoms in these ZnO nanoparticles.

#166060 - $15.00 USD Received 3 Apr 2012; revised 16 Apr 2012; accepted 16 Apr 2012; published 30 Apr 2012

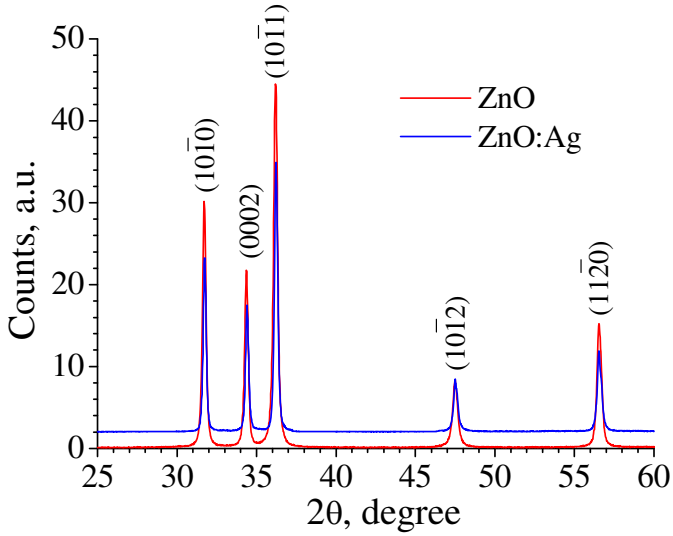

Fig. 1. XRD patterns of as prepared undoped ZnO (red line) and Ag-doped ZnO (blue line, doping level 1.0 mol%) nanopowders. XRD were recorded using a CuKα line. Bravais-Miller indices of wurtzite ZnO structure are labeled, respectively.

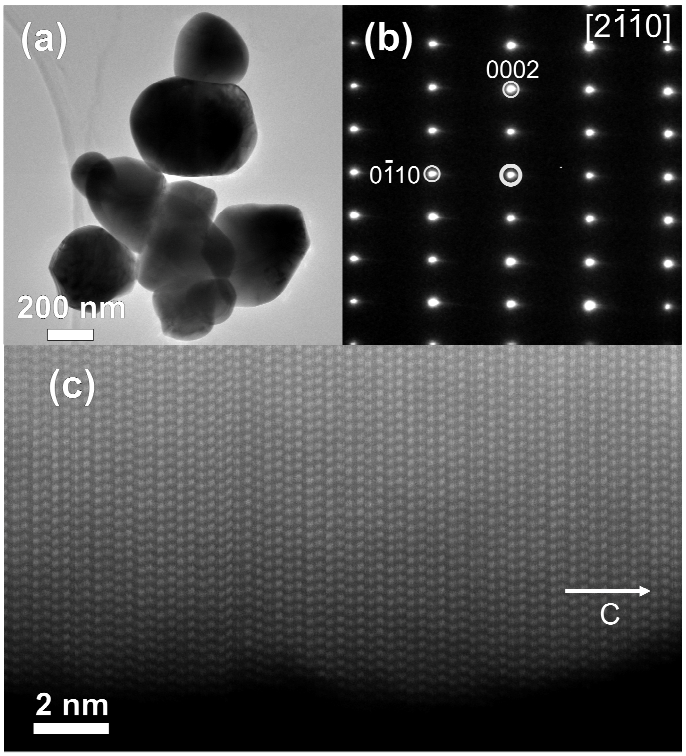

Fig. 2. (a) Low magnification bright field TEM image of Ag-doped ZnO nanoparticles; (b) the electron diffraction pattern of particles from (a) evidences the ZnO hexagonal wurtzite structure; (c) high resolution HAADF-STEM image of the edge of a ZnO nanoparticle taken along the [2$\bar{1}\bar{1}$0] zone axis; no Ag inclusions were detected.

#166060 - $15.00 USD Received 3 Apr 2012; revised 16 Apr 2012; accepted 16 Apr 2012; published 30 Apr 2012

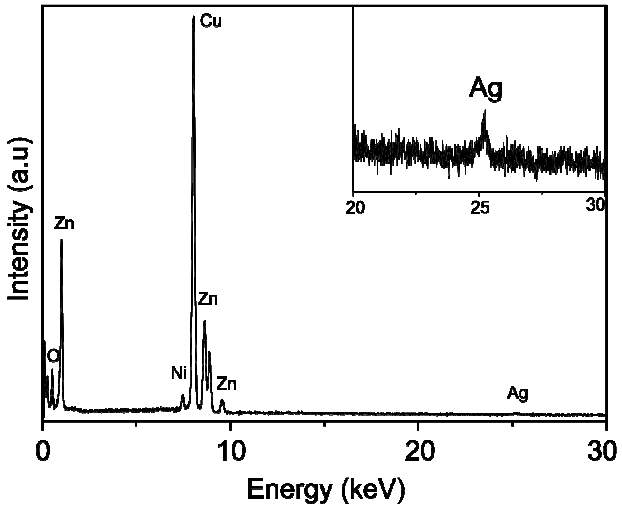

Fig. 3. TEM EDX spectrum of ZnO:Ag nanopowder, doping level 1.0 mol%, confirming doping of these sample nanopowders with silver.

The strong Cu $K\alpha_1$ line (8.048 keV) peak in Fig. 3 is due to backscattering of the incident electrons from the sample holder Cu grid and from the objective lens pole-piece of the TEM. The spectrum presented in Fig. 3 was specifically acquired from a region presented in Fig. 2 (a), only containing several Ag-doped ZnO particles. Due to low concentration of silver, the Ag peak around 25 keV is only a weak but significant feature at the given noise level, as seen in the insert to Fig. 3. The Ag-K peak situated at 25 keV significantly exceeds the noise level which confirms the presence of silver in the ZnO nanoparticles.

3.2. Photoluminescence study: low pump power regime

Figure 4 shows the emission spectra of undoped ZnO and ZnO:Ag (doping level 1.0 mol%) nanopowders excited at 355 nm into the conduction band of ZnO in the low pump power regime. The spectrum of undoped ZnO has an emission band at 545 nm, which is typical for ZnO and is generally ascribed to oxygen vacancy related defects in ZnO [1,2]. Compared to the undoped ZnO, the emission spectrum of ZnO:Ag nanopowder shows a red-shift of the green emission band. Also, the emission bands around 750 nm and 900 nm have been observed.

As discussed below the 900 nm band is split into three components. The spectra have been normalized because the scattering properties of the powders varied from sample to sample resulting in a tentative comparison of their absolute intensities. Thus, the bands at 750 and 900 nm are due to Ag dopants, and the red shift of the band at 545 nm may be assumed to be due to an extra Ag-related band/shoulder located at about 570 nm, next to the 545 nm band of the ZnO host; as will be confirmed further by the excitation spectra in Fig. 5 and in the temperature dependence studies. This band of Ag, with its emission maximum in the yellow-red part of the spectrum has been detected in a variety Ag nanoclusters doped media [15], including glasses [16,17].

The excitation spectra of the 545-570, 750 and 900 nm emission bands, which can be observed in Fig. 4, have been measured and the results are presented in Fig. 5. It is seen that the excitation spectra are similar for all three Ag–nanoclusters related emission bands when detecting at 570, 750 and 900 nm, and are dominated by an exciton absorption peak at about 380 nm with an extended short wavelength shoulder. Such excitation spectra are typical for a variety of dopants in the ZnO host, such as Li [12] or Yb [13,30], which are pumped by energy transfer from the ZnO host. Thus we conclude that these three emission bands are pumped mostly by energy transfer from the exciton state of ZnO. On the other hand, the excitation spectrum for the green emission band of the undoped ZnO host, black line in Fig. 5,

#166060 - $15.00 USD Received 3 Apr 2012; revised 16 Apr 2012; accepted 16 Apr 2012; published 30 Apr 2012

differs substantially from Ag-nanoclusters related bands; it shows only one broad band corresponding to the band-to-band transitions of the ZnO host.

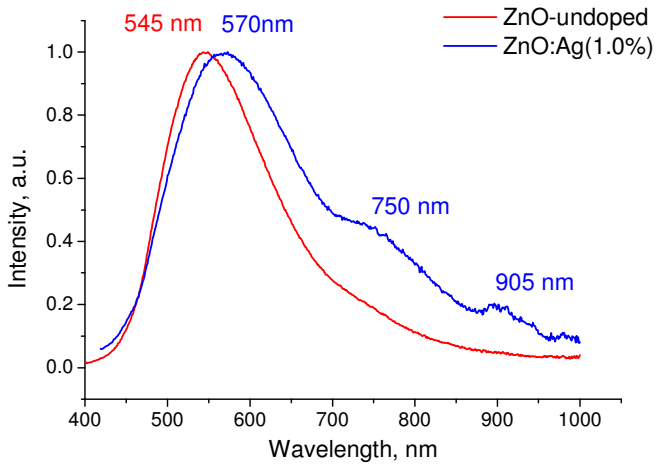

Fig. 4. Emission spectra of undoped ZnO and ZnO:Ag (1.0% doping) samples. Excitation was at 355 nm line of Ar laser in a low power regime. The estimated bands peak wavelengths are labeled, respectively.

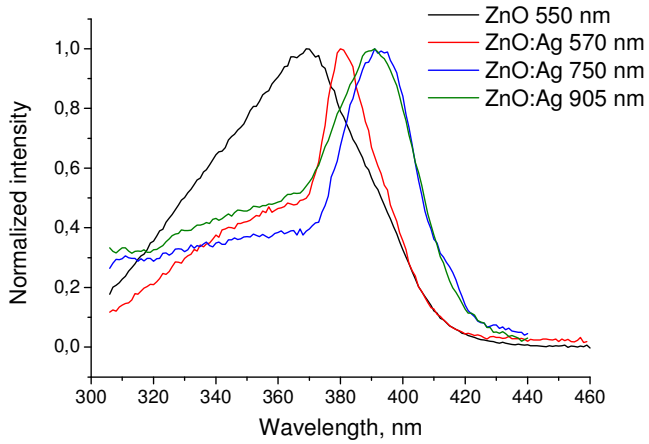

Fig. 5. Excitation spectra for three emission bands related to Ag and detected at the post-signed wavelenghts 570, 750 and 905 nm. The excitation spectrum for the intrinsic luminescence band detected at 550 nm is also shown, for comparison.

3.3. Photoluminescence study: high pump power regime

Figure 6 shows the effect of the pump power on the shape of the emission spectrum for undoped ZnO (a) and for ZnO:Ag (b) nanopowders, which have been heat treated in oxygen. It is clearly seen that, at low pump power, the bands at 750 and 900 nm become stronger with respect to the 545-570 nm band. This indicates substantially different pump power dependence for the emission bands presented in Fig. 6. We found that the 750 and 900 nm bands in the ZnO:Ag samples have sub-linear pump power dependence, which is typical e.g. of quantum cutting mechanisms for the energy transfer from the ZnO exciton state, e.g. in [12,30,31], while the green emission band has a substantially stronger pump power dependence typical of conventional linear excitation processes, e.g. in [12,30,31].

#166060 - $15.00 USD Received 3 Apr 2012; revised 16 Apr 2012; accepted 16 Apr 2012; published 30 Apr 2012

3.4. Effect of heat-treatment and temperature dependence of luminescence

To gain extra information about the origin of Ag emission bands we carried out heat-treatment of the as-prepared nanopowders, in particular in oxygen atmosphere since an effect of oxygen on the emission bands of ZnO is known [1,32,33]. The samples were heat-treated in a horizontal tube Lenton furnace in a constant flow of oxygen through the tube. During the heat-treatment the samples were held in alumina crucible at 700 °C for 2 hours. The results are shown in Fig. 7 for undoped (a) and Ag-doped (b) nanopowders. The heat-treatment results in an enhancement of the 750 nm and 900 nm bands, which were assigned to Ag dopants earlier. Note, that 750 nm emission band of undoped ZnO was shown to be related to oxygen surplus in previous works, e.g. in [1,32,33]. The effect of pump power is stronger for the oxygen heat-treated samples compared to the as prepared samples.

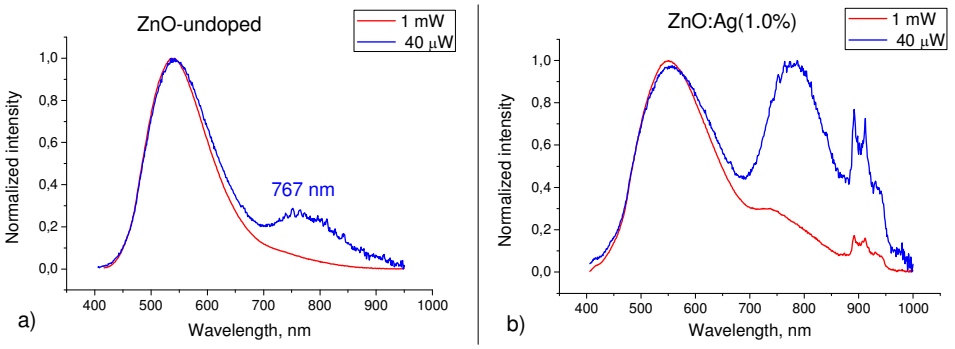

Fig. 6. Effect of excitation power on emission spectrum of (a) undoped ZnO and (b) Ag-doped ZnO nanopowders. The 355 nm line of Ar-ion laser was used for excitation; the respective pump powers are indicated. The samples were heat-treated in oxygen.

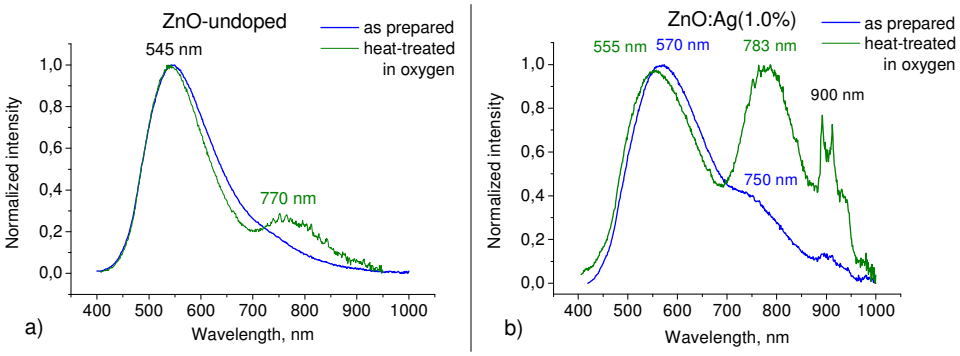

Fig. 7. Effect of heat-treatment in oxygen on emission of: (a) undoped ZnO and (b) Ag-doped ZnO:Ag (1.0% doping level) nanopowder samples. Excitation was at 355 nm in low power regime at 40 μW. Long wavelength Ag nanoclusters emission bands about 780 and 900 nm are more prominent in oxygen heat treated Ag-doped samples (b), in agreement with Fig. 6(b).

Ag doping of the ZnO nanocrystalline host was found to affect the temperature dependence of luminescence of ZnO, as seen in Fig. 8. The strongest temperature dependence was observed when detecting the green emission band at 560 nm. As it was argued above, two contributions, from the ZnO host and from the Ag dopants, will superimpose when detecting emission at this wavelength. We see that decreasing the temperature down to about 175°C results, first in an increase of emission intensity in both the undoped and the Ag-doped nanopowders. Further decrease of the temperature results in an essentially different behavior: a saturation for the undoped and decrease in emission intensity for the Ag-doped

#166060 - $15.00 USD Received 3 Apr 2012; revised 16 Apr 2012; accepted 16 Apr 2012; published 30 Apr 2012

nanopowders. This difference indicates indeed two contributions, from the ZnO host and from the Ag dopants, as proposed above in description of data of Fig. 4.

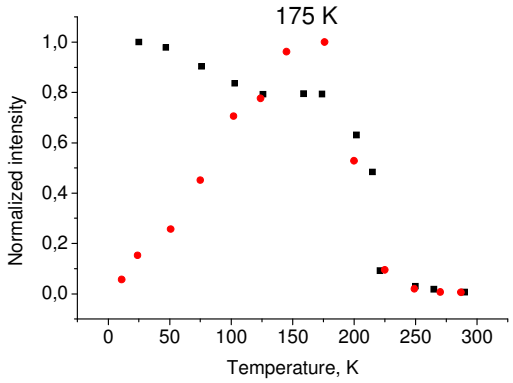

Fig. 8. Temperature dependence of the green emission band detected at 560 nm in undoped (black squares) and ZnO:Ag, 1.0% doping level, (red circles) nanopowders.

4. Discussion

4.1 The green, 540-570 nm, emission band of ZnO:Ag nanocrystals

The excitation spectra and the temperature dependence of the green emission band, shown in Figs. 5 and 8, respectively, clearly demonstrate the two contributions to the intensity of the observed green emission band of Ag-doped ZnO: the first contribution is from the ZnO host itself and the second contribution is from the Ag-dopant.

The emission band of Ag nanoclusters in the green-yellow part of the spectrum is well known for different hosts, such as zeolites, sol-gels, liquids, colloids ([15] and refs. therein) and recently we have detected this Ag nanoclusters band in a *bulk glass* host [16,17]. In the ZnO:Ag nanocrystals, this band overlaps with an intrinsic green band of the ZnO host, but based on the excitation spectra and on heat-treatment and temperature dependence data it was possible above to separate the contributions of the green-yellow luminescence of the Ag nanoclusters and the intrinsic green ZnO luminescence. An energy level diagram in Fig. 9(a) depicts a mechanism for excitation of the intrinsic emission band of ZnO (light green color): first by non-radiative relaxation of the photoexcited carriers (shown by wavy lines in Fig. 9(a)) followed by a recombination of the carriers at the oxygen vacancies; this emission process has been found to have normal linear intensity dependence [12,30,31 and refs therein]. On the other hand, the green-yellow emission band of Ag nanoclusters and its excitation by the proposed quantum cutting mechanism are indicated by the dark green color in Fig. 9(a).

The difference in temperature dependence between undoped ZnO and Ag-doped ZnO:Ag shown in Fig. 8 confirms different mechanisms for the green emission bands in these two samples. The temperature dependence of luminescence of ZnO:Ag suggests an extra mechanism of quenching of the band luminescence below 175 K. For ZnO:Ag sample, Fig. 8, transfer from CB to the ZnO exciton is suppressed below 175 K; therefore the Ag-nanoclusters related luminescence is quenched at low temperature, which confirms earlier made proposition that Ag luminescence is due to energy transfer from the exciton state of ZnO. On the other hand, the luminescence of ZnO is not quenched at low temperature, which agrees with the model of Fig. 9(a), because intrinsic luminescence of ZnO is due to relaxation of carriers directly from the conduction band.

4.2 The red, 750 nm, emission band of ZnO:Ag nanocrystals

An emission band in the region from 700 nm to 800 nm is detected both in the case of undoped and Ag-doped ZnO samples; while this band is stronger in the case of ZnO:Ag

#166060 - $15.00 USD Received 3 Apr 2012; revised 16 Apr 2012; accepted 16 Apr 2012; published 30 Apr 2012

sample. This emission band of ZnO is well known from the literature, e.g. in [1,32,33], and it was argued to be due to excess/surplus of oxygen impurities. Our data on heat-treatment in oxygen confirms this explanation. In our case, the emission band in the 700-800 nm region of the spectrum was enhanced by the heat-treatment in oxygen and by Ag-doping, indicating that this emission band is due to Ag-O clusters. The mechanism for excitation of this band is shown schematically in Fig. 9(a) in the red.

4.3. The infrared, 900 nm, emission band of Ag nanoclusters and its orbital splitting

To our knowledge, very little is known about the infrared emission of Ag-nanoclusters at about 900 nm. Recently an emission band of Gaussian-type shape in this region was reported for colloidal Ag-nanoclusters [34]. In our *nanocrystalline* samples, this band has a specific splitting in three components, which apparently is typical for the emission of transition metals in anisotropic crystalline lattices, such as wurtzite ZnO lattice in our case. Here we also note, that the 900 nm band *cannot* be due to single Ag atoms/ions, which normally emit in the UV part of the spectrum ([35] and refs. therein).

Sugano-Tanabe theory explains an orbital splitting of energy levels of transition metals, such as Ag, in a crystal field [36,37]; the split is defined by the crystal symmetry. ZnO has a hexagonal anisotropic C_{6V} symmetry point group. The charge compensation reaction for introduction of Ag in the ZnO lattice may be written according to Eq. (1); assuming that Ag^{+} replaces Zn^{2+} in its tetragonal surrounding in the ZnO.

$$V^{2+}_{Zn} = 2Ag^{+} \tag{1}$$

It is seen from Eq. (1) that essentially two Ag^{+} ions are required for the charge compensation of Zn^{2+}, and this provides a mechanism for nucleation of Ag nanoclusters in ZnO host, such as Ag dimers.

The tetragonal field is known [37] to split excited $^{3}T_{2g}$ state of transition atoms into twofold orbital degenerate E levels and a single non-degenerate level A. The ground state is A state. Such splitting of the excited and ground states correspond to the experimentally detected split for the 900 nm emission band of Ag presented in Figs. 4, 6, and 7. The two components have similar intensities as they correspond to the allowed E→A transition, while the lower energy third component has a weaker intensity as it corresponds to the forbidden A→A transition. The crystalline character of the Ag nanocluster site accounts for the experimentally detected splitting of this band. The mechanism for excitation of this band is depicted schematically in Fig. 9(a) in the black.

4.4 Optical transitions, energy level diagram and mechanism for formation of Ag-nanoclusters

The diagram in the Fig. 9(a) illustrates the mechanisms for excitation of the above presented emission bands for the undoped (light green colour) and Ag-nanoclusters doped ZnO:Ag nanopowders (dark green, red and black colours). The involved energy levels of Ag nanoclusters Ag_{CL} are labelled, respectively.

#166060 - $15.00 USD Received 3 Apr 2012; revised 16 Apr 2012; accepted 16 Apr 2012; published 30 Apr 2012

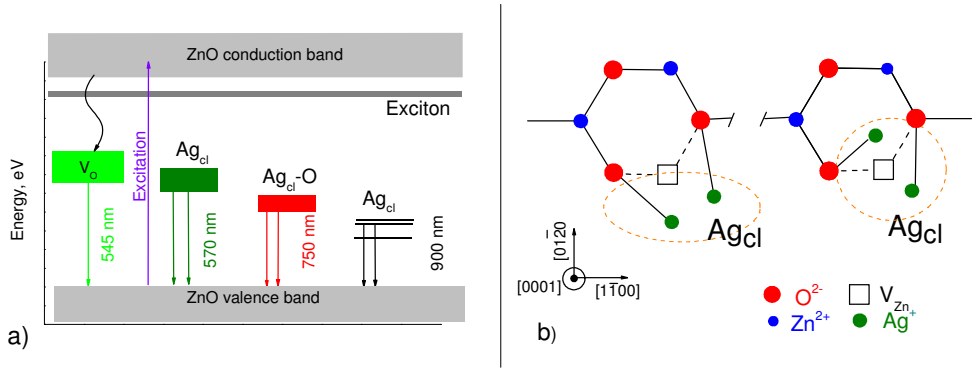

Fig. 9. (a) Schematic diagram for excitation and emission transitions for udoped and Ag-doped ZnO (see text for details); (b) two possible configurations resulting from substitution of Ag dimer onto place of one Zn^{2+} vacancy.

The emission bands near 570, 750 and 900 nm are related to the Ag-nanoclusters. They are excited by energy transfer from the ZnO exciton state through a quantum cutting process, as argued above. The temperature dependence of ZnO:Ag indicates the presence of two emission quenching mechanisms dominating below and above 175 K. Below 175 K, the emission is quenched due to a reduction of charge carrier transfer from the ZnO conduction band to the ZnO exciton level. At temperatures higher than 175 K, a well known Fröhlich mechanism of electron-phonon interaction dominates, causing the observed emission to decrease.

Figure 9(b) shows a fragment of a ZnO wurtzite structure with one Zn^{2+} ion vacancy. According to the Eq. (1), two Ag ions substitute simultaneously instead of one Zn^{2+}, resulting in an Ag-dimer. As it was shown in [17], if these nanoclusters are close enough they may form bigger Ag-nanoclusters. The shape and the size of the involved Ag-nanoclusters is a topic for our extended further research.

When the Ag-dimers locate next to each other inside the ZnO host, this promotes a cooperative quantum cutting processes [12,30,31] as deduced from the above experimental data and indicated by the two down-headed arrows in Fig. 9(a). A decaying exciton of ZnO can excite two close Ag-dimers simultaneously/cooperatively, due to the large Bohr radius of the exciton. In ZnO, the Bohr radius is R_{Bohr} = 1.4 nm [38], which is the upper limit for Ag separation of Ag dimers, which can participate in quantum cutting process. More distant Ag dimers (or nanoclusters) cannot contribute to the cooperative quantum cutting process [12], but they may contribute to a conventional linear de-excitation process.

5. Conclusion

We reported on the preparation of nanocrystalline ZnO powder doped with luminescent Ag-nanoclusters. The Ag-doping results in three emission bands near 570, 750 and 900 nm; the last band has a characteristic splitting in an anisotropic crystalline ligand field of the wurtzite structured ZnO. The detected emission bands point towards promising applications of the ZnO:Ag nanopowders, especially bearing in mind their low cost and availability. Device applications of these ZnO nanopowders doped with Ag-nanoclusters may include UV-driven white light generation in luminescent lamps, flexible displays, down-shifting of solar spectrum for enhancement of efficiency of solar cells.

Acknowledgments

We are grateful to the Methusalem Funding of Flemish Government for the support of this work. Y.-G. L. and S.T. acknowledge funding from the Fund for Scientific Research Flanders (FWO) for a postdoctoral grant and under grant number G056810N. The microscope used in this study was partially financed by the Hercules Foundation. J.V. acknowledges funding from the European Research Council under the 7th Framework Program (FP7), ERC grant N°246791 – COUNTATOMS and ERC Starting Grant 278510 VORTEX. The authors

acknowledge the guidance of Prof. G. Van Tendeloo, EMAT Antwerpen University, in transmission electron microscopy study in this work.

#166060 - $15.00 USD Received 3 Apr 2012; revised 16 Apr 2012; accepted 16 Apr 2012; published 30 Apr 2012